



STRUCTURAL SCIENCE
CRYSTAL ENGINEERING
MATERIALS

Volume 78 (2022)

Supporting information for article:

Electronic structure of $(\text{MePh}_3\text{P})_2[\text{Ni}^{\text{II}}(\text{bdtCl}_2)_2] \cdot 2(\text{CH}_3)_2\text{SO}$ and $(\text{MePh}_3\text{P})[\text{Ni}^{\text{III}}(\text{bdtCl}_2)_2]$, (bdtCl_2 - 3,6-dichlorobenzene-1,2-dithiolate)

Julia Adamko Koziskova, Yu-Sheng Chen, Su-Yin Grass, Yu-Chun Chuang, I-Jui Hsu, Yu Wang, Martin Lutz, Anatoliy Volkov, Peter Herich, Barbora Vénosová, Ingrid Jelemenská, Lukáš Bučinský, Martin Breza and Jozef Kožíšek

Contents

SI1. Synthesis and crystallization

SI2. Crystallographic data collection

SI3. Local XDPROP software

Table S1. Neutral and positive ion scattering curves (d-populations and Ni QTAIM data)

Table S2. Selected bond distances and angles

Table S3. B3LYP/def2-TZVP BCP characteristics of QTAIM analysis, that is, A1-BCP-A2distance d , charge density ρ , Laplacian $\Delta\rho$, ellipticity ε , Hessian eigenvalues $\lambda_1 < \lambda_2 < \lambda_3$ and DI delocalization index

Table S4. B3LYP/def2-TZVP TD-DFT Ni K-edge and S K-edge transition energies

Table S5. Weight of individual excitations in the Ni K-edge TD-DFT transitions

Table S6. Weight of individual excitations in the S K-edge TD-DFT transitions

Figure S1. Experimental residual density

Figure S2. Experimental and B3LYP/6-311G* static electron deformation densities and Laplacian maps

Figure S3. DAFH eigenvectors at B3LYP/def2-TZVP level of theory

Figure S4. Experimental static electron deformation densities and Laplacian maps

Figure S5. 3D experimental static electron deformation densities and Laplacian maps

Figure S6. Frontier orbitals of complexes studied

Figure S7. DAFH eigenvectors at different contours

Figure S8. Volume of Ni for (1) and (2)

References

SI1. Synthesis and crystallization

Complexes $(\text{MePh}_3\text{P})_2[\text{Ni}^{\text{II}}(\text{bdtCl}_2)_2] \cdot 2\text{DMSO}$ (**1**) and $(\text{MePh}_3\text{P})[\text{Ni}^{\text{III}}(\text{bdtCl}_2)_2]$ (**2**) were prepared as follows: The solution of Na (0.08 g, 3.3 mmol) in MeOH (10 ml) was added to 3,6-dichlorobenzene-1,2-dithiol (bdtCl₂; 0.34 g, 1.6 mmol). To this mixture, a solution of NiCl₂.6H₂O (0.18 g, 0.76 mmol) in MeOH (10 ml) was added. Finally, a solution of methyltriphenylphosphonium bromide ($\text{CH}_3\text{P}(\text{C}_6\text{H}_5)_3\text{Br}$; 0.57 g, 1.6 mmol) in MeOH (10 ml) was added. The resulting solution was stirred for 20 min. The complexes were precipitated by fast addition of water, accompanied by vigorous stirring. The raw product (dark yellow-green crystalline powder) was filtered off and washed with diethylether. The complex (**1**) is insoluble (yellow-brown powder) and the complex (**2**) was isolated from crude product with acetone (as green solution). The complex (**1**) was recrystallized from DMSO/H₂O solution (1:10) (yield 46 %) and the complex (**2**) was recrystallized from acetone/methanol solution (40:5) (yield 54 %). After recrystallization, suitable crystals were selected for the X-ray diffraction experiments. All reagents were from Sigma-Aldrich (p.a. grade) and solvents were products of mikroCHEM (p.a. grade). Synthesis in an inert atmosphere gives purely complex (**1**).

SI2. Crystallographic data collection

The data were collected at 100.0(1) K on a Eulerian 4-circle Stoe STADIVARI diffractometer with a Dectris Pilatus 300K detector, Incoatec I μ S Ag microfocus source (Ag-K α , $\lambda = 0.56083 \text{ \AA}$) at 100 K using a nitrogen gas open-flow Cobra cooling system from Oxford Cryosystems. For (**1**) two detector positions for 42 omega scans ($2\theta = -30.6^\circ$ and 30.9°) with a frame width of 0.25° were used. The exposure time for each frame was of 200 seconds. The maximum resolution reached at this experimental setting was $d = 0.4367 \text{ \AA}$ and $\sin(\theta)/\lambda = 1.14485 \text{ \AA}^{-1}$. For (**2**) also two detector positions for 42 omega scans ($2\theta = -28.6^\circ$ and 28.9°) with a frame width of 0.20° were used. The exposure time for each frame was of 167 seconds. The maximum resolution reached at this experimental setting was $d = 0.4445 \text{ \AA}$ and $\sin(\theta)/\lambda = 1.12487 \text{ \AA}^{-1}$. Data reduction was performed using X-Area Integrate 1.73.1 and X-Area X-Red32 1.65.0.0 (Stoe & Cie GmbH, 2018). The absorption correction procedure employed the crystal-shape models with 10 (**1**) and 8 (**2**) faces, respectively. The average redundancy for (**1**) was of 13.0, R_{int} and R_σ were 0.0460 and 0.0231, respectively, and, for (**2**) it was of 17.8, R_{int} and R_σ were 0.0303 and 0.0134, respectively. Upon the data reduction, we have obtained direction cosines and TBAR (distance of primary and diffracted beam through the crystal) as described previously (Kožíšek *et al.*, 2002, Herich *et al.*, 2018). The details of the X-ray diffraction experiment conditions and the crystallographic data are given in **Table 1**. As the symmetry-equivalent data were collected with different TBAR values, all non-averaged data were used in the refinements.

Additional synchrotron data for the Ni(III) complex (**2**, 15 K) were collected at the Advanced Photon Source (APS). The diffraction intensities were collected by the Huber three-circle diffractometer

equipped with a Pilatus 3x CdTe 1M shutterless pixel array detector with $\lambda = 0.30996 \text{ \AA}$ at $T = 15\text{K}$ maintained by the helium open-flow Cryostream system. A φ -scan with 0.3° interval was used for data collection. Data reduction was done with EVAL15 (Schreurs *et al.*, 2010) at the resolution of 1.52 \AA^{-1} ($d = 0.3289 \text{ \AA}$).

SI3. Local XDPROP software

The local code uses a standard PROMEGA technique (Keith, T. A. & Bader, R. F. W., 1993; Gatti *et al.*, 1994; Popelier, 1998). It starts by projecting (outward from the position of an atomic nucleus) a number of integration rays defined using the Lebedev-Laikov angular grid (Lebedev & Laikov, 1999) and then steps away from the nucleus along each ray until a zero-flux surface (also known as an interatomic surface) is found. The trajectory of the gradient of the electron density (Popelier, 1998) at each step along the ray is traced using the standard 5th order Runge-Kutta algorithm with the error monitoring and adaptive step size (Press *et al.*, 1992). Radial integration employed the standard Gauss-Legendre quadrature (Press *et al.*, 1992). A typical quadrature included 200 radial and 1202 angular points, but for several atoms in each structure, it was deemed necessary to increase the number of the angular grid points to 2702 and 5810. The crystal environment was simulated by generating all symmetry-equivalent atoms with fractional coordinates $-1 \leq x_f, y_f, z_f \leq 2$. In order to speed up the calculations, the in-house version of XDPROP was parallelized using Message Passing Interface (MPI). The boundaries of the atomic basins (interatomic / zero-flux surfaces) were visualized in the ParaView 5.9.0 program (Ahrens *et al.*, 2005; Ayachit, 2015) using the 3D Delaunay triangulation technique (see Fig. S1).

Table S1

Neutral atom scattering curve for Ni ([Ar] 4s² 3d⁸), Positive cation scattering curve for Ni²⁺ ([Ar] 4s⁰ 3d⁸). N, Q and V001 values in square brackets refer to TOPXD [TOPINT] integration of the neutral atom scattering curve

Scattering curve	Monopoles (start)	GROUPS *	d _{z2} d _{xz}	d _{yz} d _{x²-y²}	d _{xy} Σ	M1(Ni) [NiS ₄ C ₁₂ Cl ₄ H ₄] ^{q+}	N (Ni) [e] Q (Ni) [e]	V001 (Ni) [Å ³] R [%]
(1) - 100 K neutral [Ar] 4s ² 3d ⁸	Ni = 4, S = 6.5, P = 4	G1 = 0, G2 = -1 G3 = +1, G4 = 0	1.95 1.84	1.82 1.83	0.84 8.28	4.1393 -2.34	27.937 [27.646] +0.063 [+0.354]	34.19 [15.13] 2.7483
(1) - 100 K Ni ²⁺ [Ar] 4s ⁰ 3d ⁸	Ni = 4 S = 7 P = 4,	G1 = -1, G2 = -2 G3 = +1, G4 = 0	2.11 1.98	1.97 1.92	0.90 8.87	4.4327 -1.78	27.067 + 0.933	14.33 2.760
(2) - 100 K neutral [Ar] 4s ² 3d ⁸	Ni = 4, S = 6.25, P = 4	G1 = 0, G2 = -1/2 G3 = -1/2, G4 = +1	2.04, 1.89 1.47, 1.89	1.99, 1.60 1.65, 1.50	0.76, 1.00 7.90, 7.89	3.9518, 3.9450 -1.24, -1.38	27.567, 27.555 [27.307 27.299] +0.433, +0.445 [+0.693, +0.701]	33.51, 33.36 [16.11. 18.58] 2.2674
(2) - 100 K Ni ²⁺ [Ar] 4s ⁰ 3d ⁸	Ni = 4 S = 6.75 P = 4	G1 = -2, G2 = -3/2 G3 = -3/2, G4 = +1	2.08, 1.94 1.52, 1.94	2.04, 1.65 1.66, 1.53	0.74, 1.02 8.04, 8.07	4.0216, 4.0361 -0.66, -0.78	26.294, 26.321 +1.706, +1.679	13.21, 13.19 2.2897
(2) - 15 K neutral [Ar] 4s ² 3d ⁸	Ni = 4, S = 6.25, P = 4	G1 = 0, G2 = -1/2 G3 = -1/2, G4 = +1	1.74, 2.03 1.60, 1.56	1.83, 1.85 1.96, 1.86	1.03, 0.74 8.16, 8.05	4.0806, 4.0237 -1.23, -1.37	27.800, 27.682 +0.200, +0.318	34.37, 34.12 2.6072
(2) - 15 K Ni ²⁺ [Ar] 4s ⁰ 3d ⁸	Ni = 4 S = 6.75 P = 4	G1 = -2, G2 = -3/2 G3 = -3/2, G4 = +1	1.73, 2.02 1.59, 1.56	1.82, 1.84 1.95, 1.85	1.03, 0.75 8.12, 8.02	4.0585, 4.0105 -0.67, -0.78	26.335, 26.239 +1.665, +1.761	12.485, 12.395 2.6073
(2) - 15 K Ni ³⁺ [Ar] 4s ⁰ 3d ⁷	Ni = 4 S = 7 P = 4	G1 = -4, G2 = -5/2 G3 = -5/2, G4 = +1	1.72, 1.91 1.34, 1.31	1.99, 1.85 2.26, 2.32	0.66, 0.46 7.98, 7.85	3.9878, 3.9247 -1.68, -1.80	26.185, 26.060 +1.815, +1.940	11.044, 10.945 2.6196

Table S2. Selected bond distances and angles

Compound (1) - 100 K; neutral [Ar] 4s ² 3d ⁸				Compound (1) - 100 K; Ni ²⁺ [Ar] 4s ⁰ 3d ⁸				
Bond	Distance, D1 [Å]	Bond angle	Angle [°]	Bond	Distance, D2 [Å]	Bond angle	Angle [°]	D1-D2/σ
Ni1-S1	2.17543(6)	S1-Ni1-S2	91.350(2)	Ni1-S1	2.17338(6)	S1-Ni1-S2	91.333(2)	34.2
Ni1-S2	2.16874(5)	S1-Ni1-S2	88.650(2)	Ni1-S2	2.17009(5)	S1-Ni1-S2	88.667(2)	-27.0
Cl1-C2	1.7424(3)	S1-Ni1-S1	180	Cl1-C2	1.7418(3)	S1-Ni1-S1	180	2.0
Cl2-C5	1.7425(3)	S2- Ni1-S2	180	Cl2-C5	1.7418(3)	S2- Ni1-S2	180	2.3
S1-C1	1.7439(3)	Ni1-S1-C1	104.579(10)	S1-C1	1.7443(3)	Ni1-S1-C1	104.569(10)	-1.3
S2-C6	1.7428(3)	Ni1-S2-C6	104.685(9)	S2-C6	1.7411(3)	Ni1-S2-C6	104.713(9)	5.7
C1-C6	1.4164(4)	Cl1-C2-C1	119.44(2)	C1-C6	1.4162(4)	Cl1-C2-C1	119.36(2)	0.5
C1-C2	1.4044(4)	Cl1-C2-C3	117.84(3)	C1-C2	1.4035(4)	Cl1-C2-C3	117.90(3)	2.3
C5-C6	1.4006(3)	Cl2-C5-C4	118.23(2)	C5-C6	1.4011(3)	Cl2-C5-C4	118.17(2)	-1.7
P1-C7	1.7818(3)	Cl2-C5-C6	119.11(2)	P1-C7	1.7836(3)	Cl2-C5-C6	119.16(2)	-6.0
Compound (2) - 100 K; neutral [Ar] 4s ² 3d ⁸				Compound (2) - 100 K; Ni ²⁺ [Ar] 4s ⁰ 3d ⁸				
Bond	Distance, D1 [Å]	Bond angle	Angle [°]	Bond	Distance, D2 [Å]	Bond angle	Angle [°]	D1-D2/σ
Ni1-S1	2.14887(4)	S1-Ni1-S2	92.7808(16)	Ni1-S1	2.14898(4)	S1-Ni1-S2	92.7829(16)	-2.8
Ni1-S2	2.13677(4)	S1-Ni1-S2	87.2192(16)	Ni1-S2	2.13685(4)	S1-Ni1-S2	87.2171(16)	-2.0
Cl1-C2	1.7374(3)	S1-Ni1-S1	180	Cl1-C2	1.7374(3)	S1-Ni1-S1	180	0.0
Cl2-C5	1.7245(3)	S2- Ni1-S2	180	Cl2-C5	1.7245(3)	S2- Ni1-S2	180	0.0
S1-C1	1.7312(2)	Ni1-S1-C1	104.007(7)	S1-C1	1.7305(2)	Ni1-S1-C1	104.004(7)	3.5
S2-C6	1.7284(2)	Ni1-S2-C	104.436(7)	S2-C6	1.7279(2)	Ni1-S2-C6	104.432(7)	2.5
C1-C6	1.4107(3)	Cl1-C2-C1	118.748(19)	C1-C6	1.4113(3)	Cl1-C2-C1	118.724(19)	-2.0
C1-C2	1.4039(3)	Cl1-C2-C3	119.510(19)	C1-C2	1.4042(3)	Cl1-C2-C3	119.52(2)	-1.0
C5-C6	1.4061(3)	Cl2-C5-C4	119.400(19)	C5-C6	1.4065(3)	Cl2-C5-C4	119.406(19)	-1.3
P1-C13	1.7923(2)	Cl2-C5-C6	119.229(19)	P1-C13	1.7924(2)	Cl2-C5-C6	119.204(19)	-0.5
Ni2-S3	2.14231(4)	S3-Ni2-S4	92.3601(15)	Ni2-S3	2.14239(4)	S3-Ni2-S4	92.3613(15)	-2.0
Ni2-S4	2.14678(4)	S3-Ni2-S4	87.6399(15)	Ni2-S4	2.14688(4)	S3-Ni2-S4	87.6387(15)	-2.5
Cl3-C8	1.7320(2)	S3-Ni2-S3	180	Cl3-C8	1.7318(2)	S3-Ni2-S3	180	1.0
Cl4-C11	1.7278(2)	S4- Ni2-S4	180	Cl4-C11	1.7276(2)	S4- Ni2-S4	180	1.0
S3-C7	1.7353(2)	Ni2-S3-C7	104.882(7)	S3-C7	1.7350(2)	Ni2-S3-C7	104.881(7)	1.5
S4-C12	1.7366(2)	Ni2-S4-C12	104.707(7)	S4-C12	1.7362(2)	Ni2-S4-C12	104.705(7)	2.0
C7-C12	1.4105(3)	Cl3-C8-C7	119.645(18)	C7-C12	1.4109(3)	Cl3-C8-C7	119.644(18)	-1.3
C7-C8	1.4079(3)	Cl3-C8-C9	118.942(18)	C7-C8	1.4080(3)	Cl3-C8-C9	118.936(18)	-0.3
C11-C12	1.4079(3)	Cl4-C11-C10	118.923(19)	C11-C12	1.4081(3)	Cl4-C11-C10	118.923(18)	-0.7
		Cl4-C11-C12	119.764(18)			Cl4-C11-C12	119.763(17)	

Compound (2) - 15 K; neutral [Ar] 4s ² 3d ⁸				Compound (2) - 15 K; Ni ²⁺ [Ar] 4s ⁰ 3d ⁸				
Bond	Distance, D1 [Å]	Bond angle	Angle [°]	Bond	Distance, D2 [Å]	Bond angle	Angle [°]	D1-D2/σ
Ni1-S1	2.15856(6)	S1-Ni1-S2	92.813(2)	Ni1-S1	2.15856(6)	S1-Ni1-S2	92.813(2)	0.0
Ni1-S2	2.14106(6)	S1-Ni1-S2	87.187(2)	Ni1-S2	2.14107(6)	S1-Ni1-S2	87.187(2)	-0.2
C11-C2	1.7438(3)	S1-Ni1-S1	180	C11-C2	1.7439(3)	S1-Ni1-S1	180	-0.3
C12-C5	1.7302(3)	S2- Ni1-S2	180	C12-C5	1.7302(3)	S2- Ni1-S2	180	0.0
S1-C1	1.7339(2)	Ni1-S1-C1	103.998(9)	S1-C1	1.7339(2)	Ni1-S1-C1	103.998(9)	0.0
S2-C6	1.7367(2)	Ni1-S2-C6	104.373(9)	S2-C6	1.7366(2)	Ni1-S2-C6	104.373(9)	0.5
C1-C6	1.4166(3)	C11-C2-C1	118.89(2)	C1-C6	1.4166(4)	C11-C2-C1	118.88(2)	0.0
C1-C2	1.4102(3)	C11-C2-C3	119.49(2)	C1-C2	1.4102(3)	C11-C2-C3	119.49(2)	0.0
C5-C6	1.4086(3)	C12-C5-C4	119.60(2)	C5-C6	1.4087(3)	C12-C5-C4	119.60(2)	-0.3
P1-C13	1.8017(3)	C12-C5-C6	119.17(2)	P1-C13	1.8016(3)	C12-C5-C6	119.16(2)	0.3
Ni2-S3	2.14621(6)	S3-Ni2-S4	92.216(2)	Ni2-S3	2.14621(6)	S3-Ni2-S4	92.216(2)	0.0
Ni2-S4	2.15556(6)	S3-Ni2-S4	87.784(2)	Ni2-S4	2.15556(6)	S3-Ni2-S4	87.784(2)	0.0
C13-C8	1.7351(3)	S3-Ni2-S3	180	C13-C8	1.7351(3)	S3-Ni2-S3	180	0.0
C14-C11	1.7313(3)	S4- Ni2-S4	180	C14-C11	1.7313(3)	S4- Ni2-S4	180	0.0
S3-C7	1.7436(2)	Ni2-S3-C7	104.973(8)	S3-C7	1.7436(2)	Ni2-S3-C7	104.973(8)	0.0
S4-C12	1.7409(2)	Ni2-S4-C12	104.912(8)	S4-C12	1.7409(2)	Ni2-S4-C12	104.911(8)	0.0
C7-C12	1.4138(3)	C13-C8-C7	119.611(19)	C7-C12	1.4138(3)	C13-C8-C7	119.610(19)	0.0
C7-C8	1.4118(3)	C13-C8-C9	118.982(18)	C7-C8	1.4119(3)	C13-C8-C9	118.983(18)	-0.3
C11-C12	1.4143(3)	C14-C11-C10	118.788(19)	C11-C12	1.4144(3)	C14-C11-C10	118.788(19)	-0.3
		C14-C11-C12	119.864(18)			C14-C11-C12	119.862(18)	

Table S3. B3LYP/def2-TZVP BCP characteristics of QTAIM analysis, that is, A1-BCP-A2distance d , charge density ρ , Laplacian $\Delta\rho$, ellipticity ε , Hessian eigenvalues $\lambda_1 < \lambda_2 < \lambda_3$ and DI delocalization index

A1	A2	d [Å]	ρ [e/Å ³]	Δρ [e/Å ⁵]	ε	λ₁ [e/Å ⁵]	λ₂ [e/Å ⁵]	λ₃ [e/Å ⁵]	DI
(1)									
Ni1	S4	2.176	0.640	4.824	0.023	-2.268	-2.217	9.309	0.829
S5	Ni1	2.169	0.650	4.874	0.021	-2.313	-2.265	9.452	0.836
C7	Cl2	1.742	1.354	-7.876	0.084	-8.008	-7.386	7.517	1.079
S5	C11	1.743	1.386	-10.421	0.194	-7.354	-6.157	3.090	1.262
C10	C9	1.393	2.141	-22.428	0.263	-16.837	-13.329	7.738	1.343
C10	C11	1.400	2.119	-21.972	0.239	-16.509	-13.321	7.858	1.307
C6	S4	1.743	1.385	-10.402	0.194	-7.354	-6.157	3.109	1.264
C11	C6	1.417	2.053	-21.049	0.160	-15.587	-13.435	7.973	1.226
C8	C7	1.391	2.153	-22.690	0.258	-16.993	-13.504	7.807	1.342
C6	C7	1.405	2.098	-21.556	0.238	-16.287	-13.156	7.886	1.304
C8	H12	1.082	1.919	-24.191	0.034	-18.559	-17.946	12.313	0.959
C9	C8	1.395	2.129	-22.188	0.226	-16.566	-13.509	7.888	1.375
Cl3	C10	1.744	1.349	-7.796	0.086	-7.980	-7.348	7.532	1.078
H13	C9	1.083	1.910	-23.949	0.033	-18.420	-17.828	12.299	0.961
(2)									
Ni1	S4	2.177	0.657	4.358	0.010	-2.469	-2.445	9.272	0.892
S5	Ni1	2.169	0.667	4.406	0.009	-2.520	-2.497	9.422	0.900
C7	Cl2	1.741	1.367	-7.948	0.075	-8.097	-7.529	7.679	1.097
S5	C11	1.742	1.399	-10.619	0.175	-7.662	-6.520	3.564	1.247
C10	C9	1.392	2.146	-22.518	0.256	-16.859	-13.420	7.762	1.362
C10	C11	1.400	2.124	-22.170	0.233	-16.599	-13.467	7.897	1.295
C6	S4	1.743	1.398	-10.590	0.176	-7.654	-6.507	3.571	1.251
C11	C6	1.417	2.053	-20.943	0.175	-15.632	-13.299	7.988	1.243
C8	C7	1.392	2.158	-22.776	0.251	-17.011	-13.593	7.828	1.361
C6	C7	1.405	2.103	-21.751	0.231	-16.370	-13.302	7.921	1.292
C8	H12	1.082	1.936	-24.753	0.026	-18.976	-18.488	12.711	0.949
C9	C8	1.395	2.138	-22.496	0.206	-16.631	-13.794	7.929	1.361
Cl3	C10	1.743	1.362	-7.863	0.077	-8.063	-7.488	7.689	1.096
H13	C9	1.083	1.927	-24.516	0.025	-18.838	-18.373	12.695	0.951

Table S4. B3LYP/def2-TZVP TD-DFT Ni K-edge and S K-edge transition energies for 25 excitations (all values are in eV).

State	Ni K-edge		S K-edge	
	(1)	(2)	(1)	(2)
1	8323.982	8324.373	2430.909	2429.382
2	8328.346	8325.278	2431.469	2430.532
3	8328.477	8325.293	2431.797	2430.900
4	8328.609	8329.962	2431.995	2432.203
5	8328.658	8329.982	2432.143	2432.274
6	8328.720	8330.107	2432.214	2432.534
7	8329.120	8330.168	2432.555	2432.585
8	8329.788	8330.228	2433.021	2432.664
9	8329.824	8330.269	2433.323	2432.803
10	8329.825	8330.314	2433.507	2432.886
11	8330.251	8330.338	2433.609	2432.941
12	8330.420	8330.378	2433.832	2432.952
13	8330.818	8330.391	2433.991	2433.006
14	8330.877	8331.117	2434.218	2433.640
15	8330.886	8331.124	2434.343	2433.651
16	8331.278	8331.409	2434.847	2434.125
17	8331.767	8331.426	2435.195	2434.138
18	8331.831	8331.738	2435.338	2434.254
19	8332.071	8331.744	2435.707	2434.277
20	8332.225	8331.818	2435.812	2434.352
21	8332.394	8331.821	2435.895	2434.409
22	8332.460	8332.262	2435.980	2434.493
23	8332.782	8332.271	2436.039	2434.559
24	8332.806	8332.512	2436.117	2435.060
25	8332.838	8332.539	2436.355	2435.069

Table S5. Weights of individual excitations in the Ni K-edge TD-DFT transitions (MO numbering refers to the original value in ORCA 4.2.0, i.e. the MO numbering starts at 0)

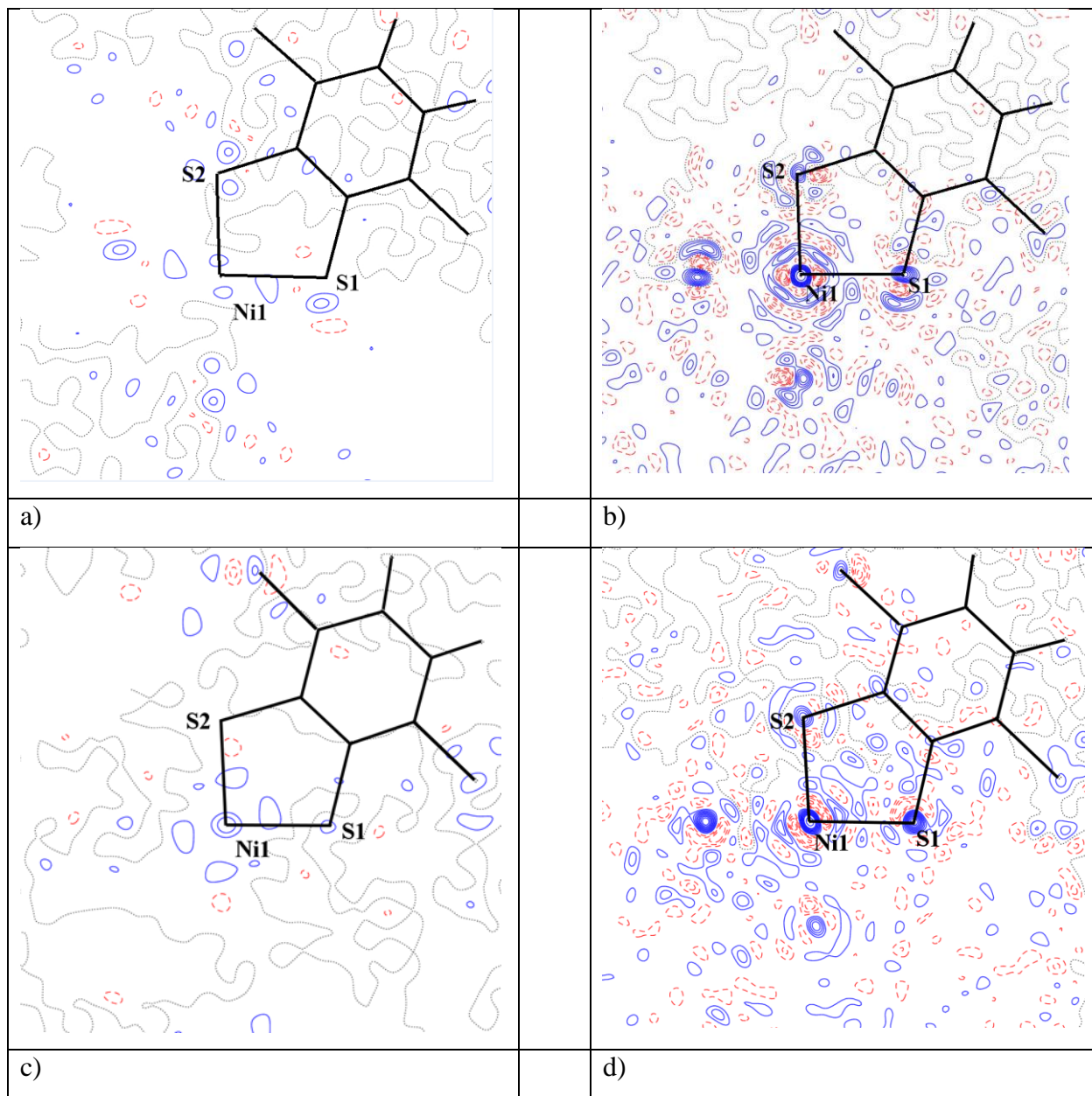
STATE	(1)	(2)
STATE 1:	119a : 0.974994 (c= 0.98741804)	118b : 0.980641 (c= -0.99027342)
STATE 2:	121a : 0.991443 (c= -0.99571234)	119a : 0.737630 (c= -0.85885363)
STATE 3:	120a : 0.998563 (c= -0.99928100)	119a : 0.247053 (c= -0.49704468) 119b : 0.735710 (c= -0.85773510)
STATE 4:	122a : 0.999685 (c= -0.99984227)	121a : 0.992742 (c= 0.99636459)
STATE 5:	123a : 0.997131 (c= -0.99856428)	121b : 0.991860 (c= -0.99592160)
STATE 6:	124a : 0.943856 (c= 0.97152247) 128a : 0.017341 (c= 0.13168609) 133a : 0.028854 (c= -0.16986388)	120a : 0.997516 (c= -0.99875747)
STATE 7:	125a : 0.992362 (c= 0.99617376)	120b : 0.997420 (c= -0.99870916)
STATE 8:	126a : 0.997272 (c= -0.99863505)	122a : 0.999846 (c= -0.99992301)
STATE 9:	130a : 0.960743 (c= 0.98017499) 146a : 0.011429 (c= 0.10690611)	123a : 0.997205 (c= -0.99860137)
STATE 10:	127a : 0.995167 (c= -0.99758058)	122b : 0.994429 (c= 0.99721078)
STATE 11:	124a : 0.031642 (c= -0.17788272) 128a : 0.895978 (c= 0.94656104) 133a : 0.070414 (c= -0.26535588)	123b : 0.997066 (c= -0.99853184)
STATE 12:	129a : 0.993227 (c= -0.99660778)	124a : 0.900475 (c= -0.94893378) 128a : 0.026372 (c= 0.16239424) 129a : 0.021791 (c= -0.14761871) 132a : 0.024751 (c= 0.15732527) 124b : 0.018836 (c= -0.13724537)
STATE 13:	131a : 0.936416 (c= -0.96768590) 134a : 0.061340 (c= -0.24766908)	124a : 0.019233 (c= 0.13868309) 124b : 0.895942 (c= -0.94654210) 128b : 0.026525 (c= 0.16286639) 129b : 0.022800 (c= 0.15099762) 132b : 0.027577 (c= -0.16606321)
STATE 14:	132a : 0.997351 (c= -0.99867473)	125a : 0.991744 (c= -0.99586325)
STATE 15:	124a : 0.016908 (c= -0.13002977) 128a : 0.085365 (c= -0.29217211) 133a : 0.873783 (c= -0.93476383) 146a : 0.011035 (c= -0.10504991)	125b : 0.991818 (c= -0.99590081)
STATE 16:	131a : 0.062560 (c= 0.25012064) 134a : 0.932222 (c= -0.96551630)	128a : 0.340663 (c= 0.58366302) 124b : 0.016251 (c= 0.12747780) 128b : 0.594965 (c= 0.77133973)
STATE 17:	143a : 0.994688 (c= 0.99734041)	124a : 0.014284 (c= -0.11951500) 128a : 0.598899 (c= -0.77388543) 128b : 0.344358 (c= 0.58682010)
STATE 18:	135a : 0.964435 (c= 0.98205637) 142a : 0.017372 (c= 0.13180442) 144a : 0.012566 (c= -0.11209680)	126a : 0.978600 (c= -0.98924221) 131a : 0.013684 (c= 0.11697820)

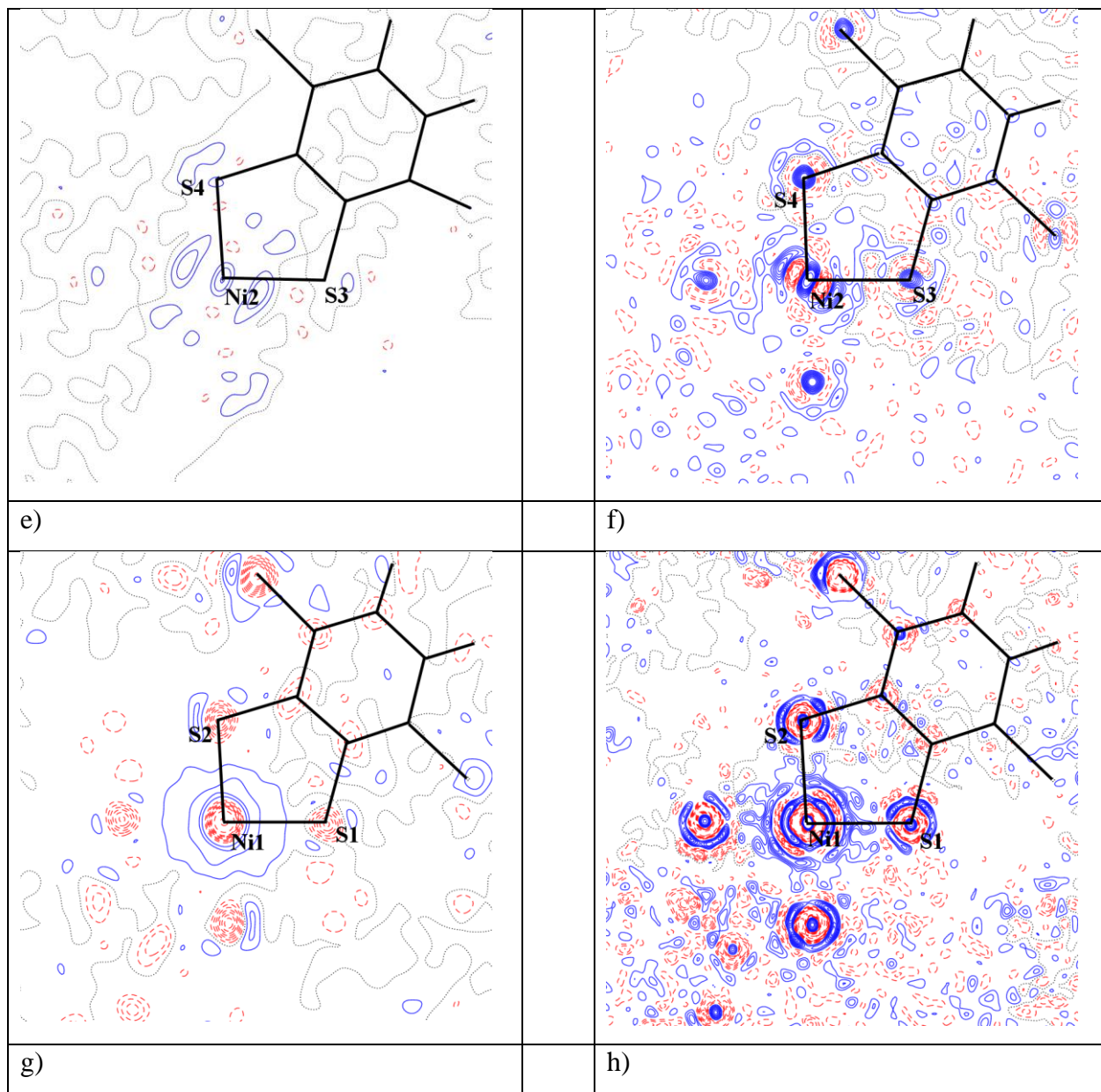
STATE 19:	136a : 0.989781 (c= 0.99487721)	126b : 0.980643 (c= 0.99027414) 131b : 0.011456 (c= 0.10703350)
STATE 20:	137a : 0.654621 (c= 0.80908648) 141a : 0.186315 (c= 0.43164232) 146a : 0.140918 (c= 0.37539016)	127a : 0.999183 (c= 0.99959159)
STATE 21:	138a : 0.996964 (c= 0.99848062)	127b : 0.998902 (c= -0.99945108)
STATE 22:	130a : 0.022860 (c= -0.15119401) 137a : 0.324660 (c= -0.56978946) 141a : 0.466608 (c= 0.68308739) 146a : 0.174851 (c= 0.41815159)	124a : 0.051398 (c= 0.22671097) 129a : 0.664768 (c= -0.81533336) 132a : 0.272151 (c= 0.52168132)
STATE 23:	135a : 0.029957 (c= -0.17308211) 142a : 0.597965 (c= 0.77328228) 144a : 0.362652 (c= -0.60220559)	124b : 0.054005 (c= 0.23238935) 129b : 0.654828 (c= 0.80921470) 132b : 0.280714 (c= -0.52982404)
STATE 24:	139a : 0.990400 (c= -0.99518859)	126a : 0.019813 (c= -0.14075827) 131a : 0.791025 (c= -0.88939590) 134a : 0.186300 (c= -0.43162527)
STATE 25:	140a : 0.989618 (c= 0.99479567)	126b : 0.017755 (c= -0.13324844) 131b : 0.761466 (c= 0.87262039) 134b : 0.217802 (c= 0.46669315)

Table S6. Weights of individual top 10 excitations in the S K-edge TD-DFT transitions (MO numbering refers to the original value in ORCA 4.2.0, i.e. the MO numbering starts at 0)

STATE	(1)	(2)
STATE 1:	119a : 0.991139 (c= 0.99555952) 120a : 0.254992 (c= -0.50496723) 121a : 0.313036 (c= 0.55949636) 122a : 0.205956 (c= 0.45382339) 123a : 0.213601 (c= 0.46216986)	118b : 0.983819 (c= 0.99187667) 119a : 0.964012 (c= 0.98184127) 119b : 0.026737 (c= -0.16351515)
STATE 3:	120a : 0.379778 (c= -0.61626126) 121a : 0.303938 (c= -0.55130584) 122a : 0.160255 (c= 0.40031922) 123a : 0.155429 (c= -0.39424476)	119a : 0.027437 (c= 0.16564228) 119b : 0.963856 (c= 0.98176163)
STATE 4:	124a : 0.699939 (c= 0.83662354) 125a : 0.196067 (c= 0.44279456) 126a : 0.016222 (c= 0.12736467) 128a : 0.018898 (c= 0.13746953) 133a : 0.017281 (c= -0.13145591) 134a : 0.013043 (c= -0.11420655)	120a : 0.166905 (c= -0.40853983) 121a : 0.351286 (c= 0.59269344) 122a : 0.147704 (c= -0.38432245) 123a : 0.213912 (c= 0.46250598) 120b : 0.017922 (c= 0.13387428) 121b : 0.044126 (c= -0.21006162) 122b : 0.016332 (c= 0.12779813) 123b : 0.026439 (c= 0.16260226)
STATE 5:	120a : 0.315709 (c= 0.56188031) 121a : 0.092633 (c= -0.30435598) 122a : 0.514793 (c= 0.71749053) 123a : 0.075838 (c= 0.27538774)	120a : 0.023609 (c= 0.15365086) 121a : 0.042728 (c= -0.20670754) 122a : 0.017982 (c= 0.13409558) 123a : 0.023107 (c= -0.15200937) 120b : 0.167372 (c= 0.40911161) 121b : 0.371421 (c= -0.60944294) 122b : 0.132748 (c= 0.36434586) 123b : 0.200400 (c= 0.44766099)
STATE 6:	120a : 0.047703 (c= 0.21841038) 121a : 0.285240 (c= 0.53407836) 122a : 0.116275 (c= 0.34099050) 123a : 0.550102 (c= -0.74168831)	120a : 0.419797 (c= -0.64791708) 121a : 0.255947 (c= -0.50591173) 122a : 0.221650 (c= -0.47079770) 123a : 0.102154 (c= -0.31961551)
STATE 7:	124a : 0.223153 (c= 0.47239049) 125a : 0.761197 (c= -0.87246603)	120b : 0.450078 (c= -0.67087867) 121b : 0.252329 (c= -0.50232398) 122b : 0.210037 (c= -0.45829838) 123b : 0.087191 (c= 0.29528175)
STATE 8:	124a : 0.016319 (c= 0.12774679) 125a : 0.025246 (c= 0.15889030) 126a : 0.534981 (c= -0.73142380) 127a : 0.411838 (c= 0.64174614)	124a : 0.383817 (c= 0.61952995) 125a : 0.061112 (c= -0.24720942) 126a : 0.010161 (c= 0.10080126) 129a : 0.016868 (c= 0.12987669) 131a : 0.018466 (c= -0.13588988) 132a : 0.014086 (c= -0.11868504) 124b : 0.312453 (c= 0.55897512) 125b : 0.052424 (c= -0.22896345)

STATE 9:	126a : 0.418214 (c= 0.64669499)	129b : 0.014162 (c= -0.11900433)
	127a : 0.563974 (c= 0.75098174)	131b : 0.014441 (c= 0.12017141)
STATE 10:	124a : 0.045003 (c= 0.21213798)	132b : 0.012519 (c= 0.11189011)
	126a : 0.026382 (c= 0.16242469)	124a : 0.343476 (c= -0.58606831)
	128a : 0.488234 (c= -0.69873726)	125a : 0.046646 (c= 0.21597614)
	129a : 0.106993 (c= 0.32709858)	129a : 0.010679 (c= -0.10333859)
	130a : 0.118627 (c= -0.34442214)	131a : 0.010306 (c= 0.10151808)
	133a : 0.096550 (c= 0.31072548)	124b : 0.411552 (c= 0.64152346)
	134a : 0.065339 (c= 0.25561464)	125b : 0.059371 (c= -0.24366214)
	144a : 0.011800 (c= 0.10862604)	129b : 0.013329 (c= -0.11545254)
		131b : 0.011920 (c= 0.10917819)
		132b : 0.010662 (c= 0.10325735)
		120a : 0.327825 (c= 0.57255969)
		121a : 0.092475 (c= -0.30409664)
		122a : 0.469112 (c= -0.68491734)
		123a : 0.108186 (c= 0.32891616)





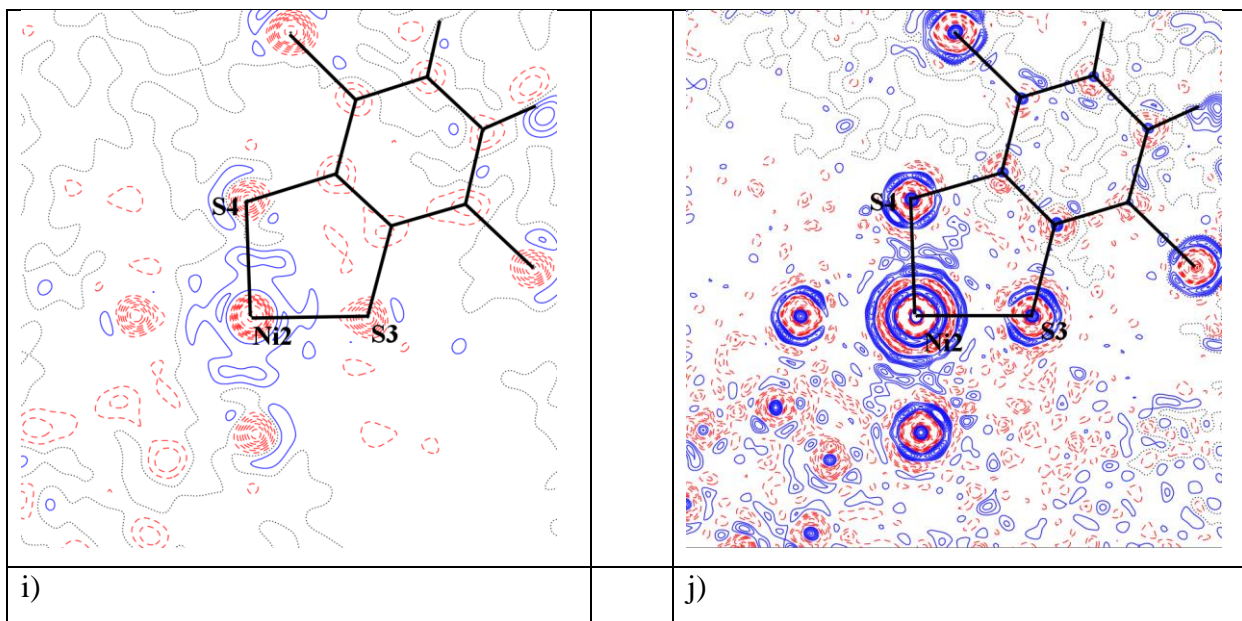
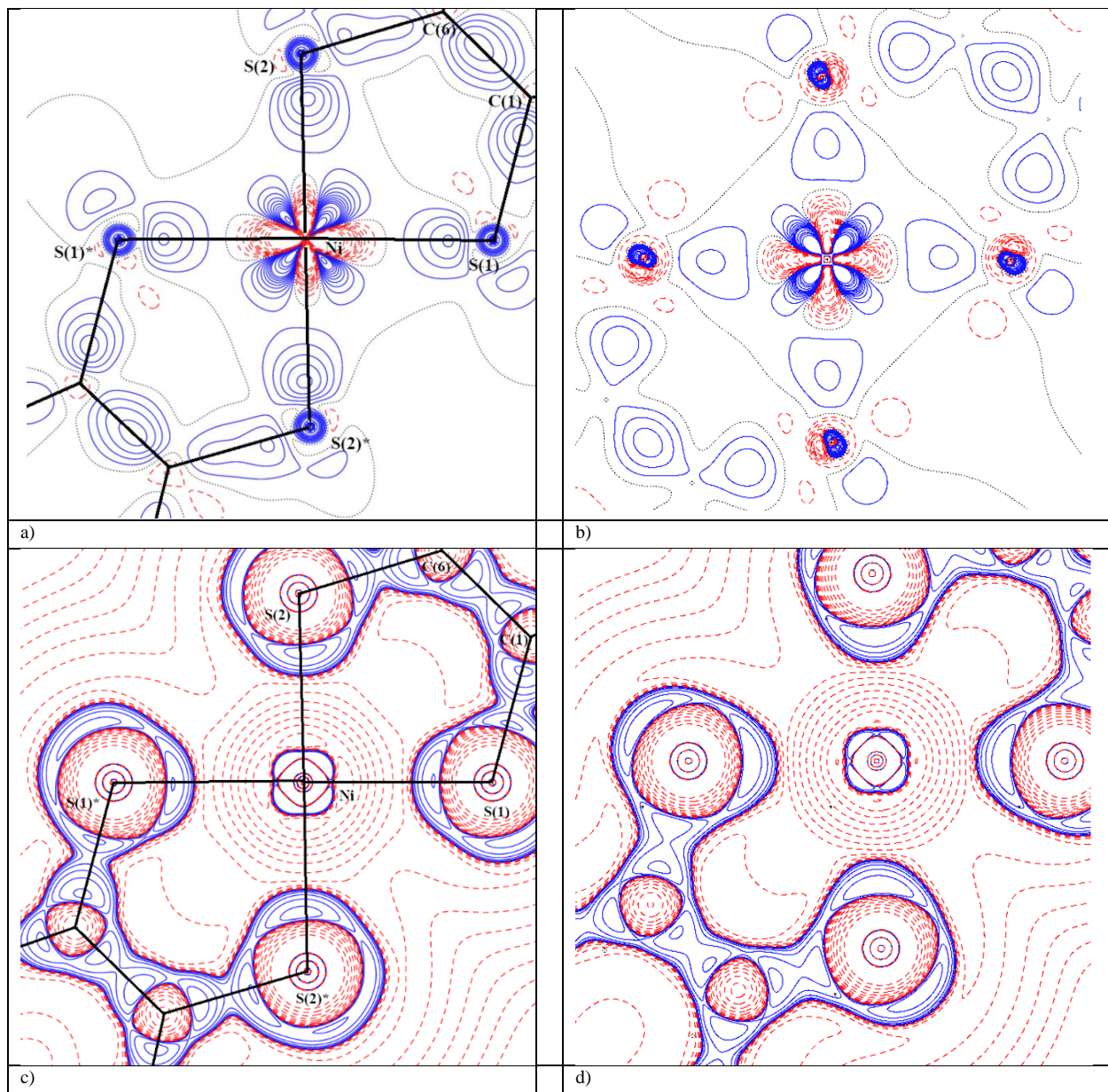


Figure S1. Experimental residual densities in the plane defined by the Ni1-S1-S2 and Ni2-S3-S4 atoms, respectively. Contour spacing 0.1 e/Å³ (positive contours - solid blue line, negative contours - dashed red line). a) for (1), resolution 0.8 Å; b) for (1), all data; c) for (2) Ni1, resolution 0.8 Å; d) for (2) Ni1, all data; e) for (2) Ni2, resolution 0.8 Å; f) for (2) Ni2, all data; g) for (2, 15 K) Ni1 resolution 0.8 Å; h) for (2, 15 K) Ni1, all data; i) for (2, 15 K) Ni2, resolution 0.8 Å; j) for (2, 15 K) Ni2, all data.



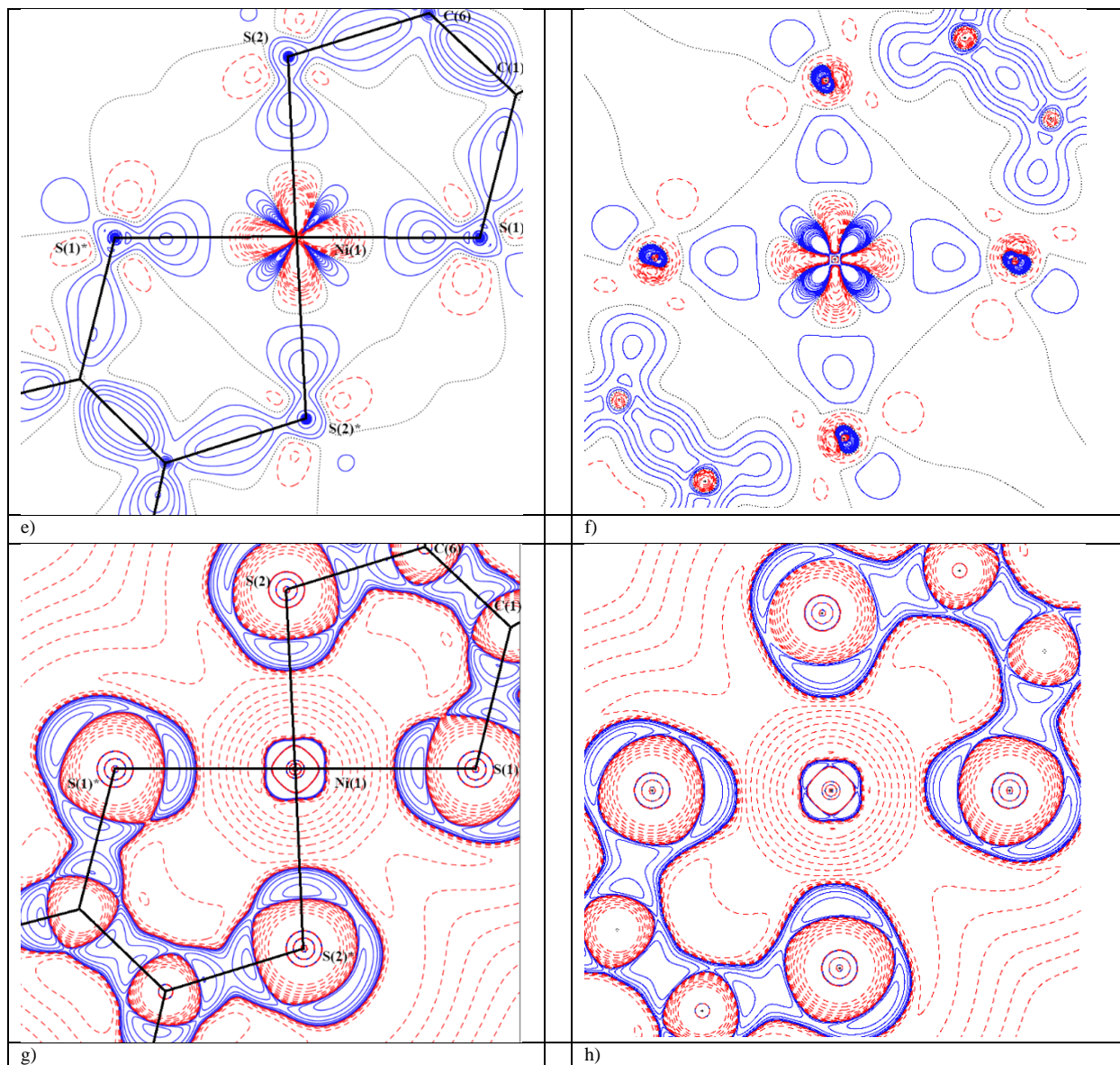


Figure S2. Experimental and B3LYP/6-311G* static electron deformation densities and Laplacian maps.

a) Experimental static electron deformation densities of (**1**) in the plane defined by the Ni1-S1-S2 atoms. Contour spacing 0.1 e/Å³, with positive contours drawn with a solid blue line and negative contours with a dashed red line. b) Theoretical static electron deformation densities of (**1**) in the plane defined by the atoms Ni1-S1-S2. Contour spacing as in a). c) Experimental Laplacian distribution $L(r) \approx \nabla^2 \rho(r)$ of (**1**) in the Ni1-S1-S2 plane. The contours are drawn at -1.0×10^{-3} , $\pm 2.0 \times 10^n$, $\pm 4.0 \times 10^n$, $\pm 8.0 \times 10^n$ ($n = -3, -2, -1, 0, +1, +2, +3$) e/Å⁵, with positive contours drawn with a solid blue line and negative contours with a dashed red line. d) Theoretical Laplacian distribution $L(r) \approx \nabla^2 \rho(r)$ of (**1**) in the Ni1-S1-S2 plane, the contours are drawn as in c). e) Experimental static electron deformation densities of (**2**) in the plane defined by the atoms Ni1-S1-S2. Contour spacing as in a). f) Theoretical static electron deformation densities of (**2**) in the plane

defined by the atoms Ni1-S1-S2. Contour spacing as in a). g) Experimental Laplacian distribution $L(r) \approx \nabla^2 \rho(r)$ of (2) in the Ni1-S1-S2 plane; the contours are drawn as in c). h) Theoretical Laplacian distribution $L(r) \approx \nabla^2 \rho(r)$ of (2) in the Ni1-S1-S2 plane. Contours are drawn as in c).

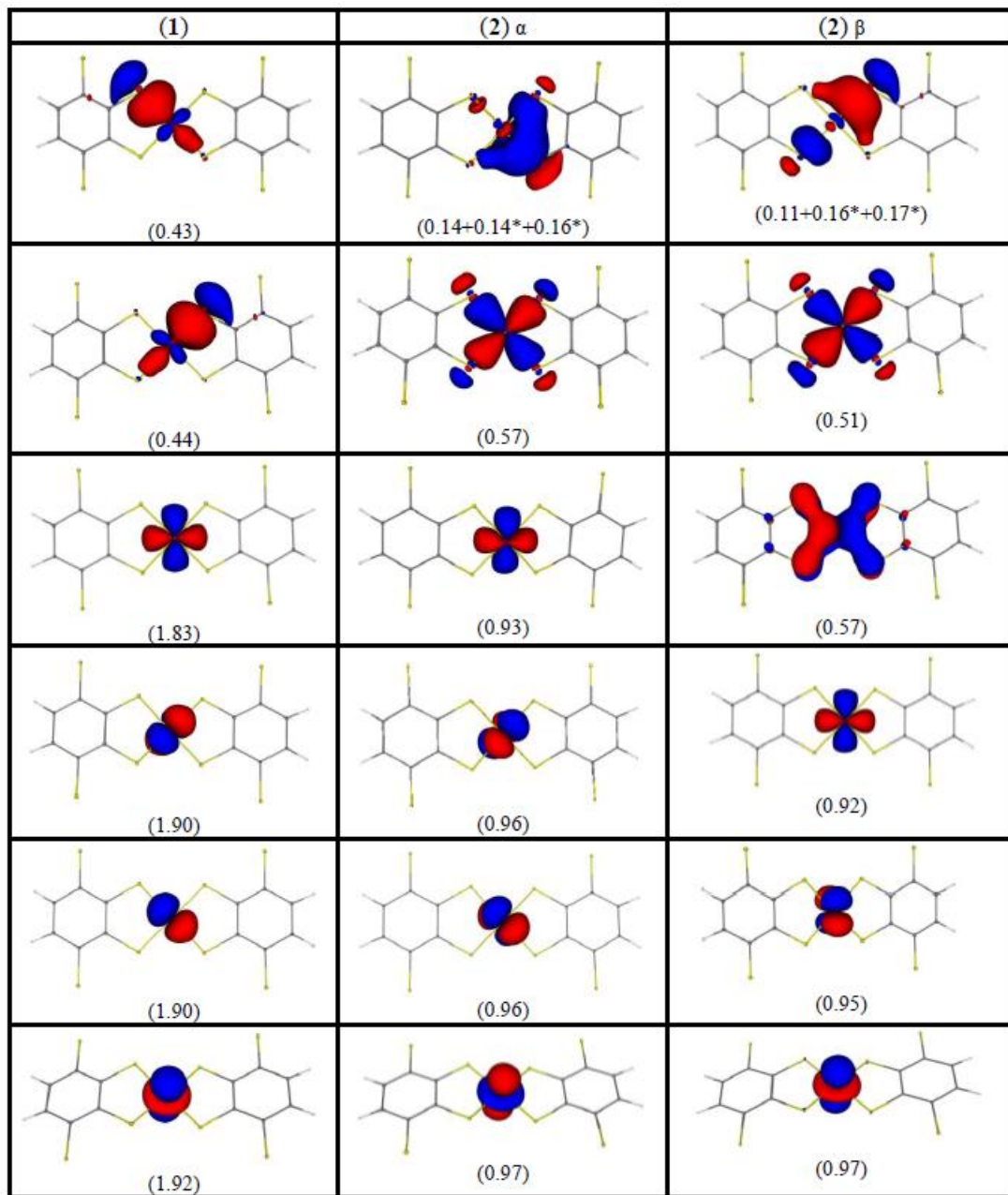


Figure S3. DAFH eigenvectors at B3LYP/def2-TZVP level of theory (isovalue 0.04, red – negative, blue – positive). Ni atoms are chosen as the domain. The DAFH eigenvalues for the Ni basin/domain are shown in parentheses (* denotes eigenvectors presented in **Fig. S7**).

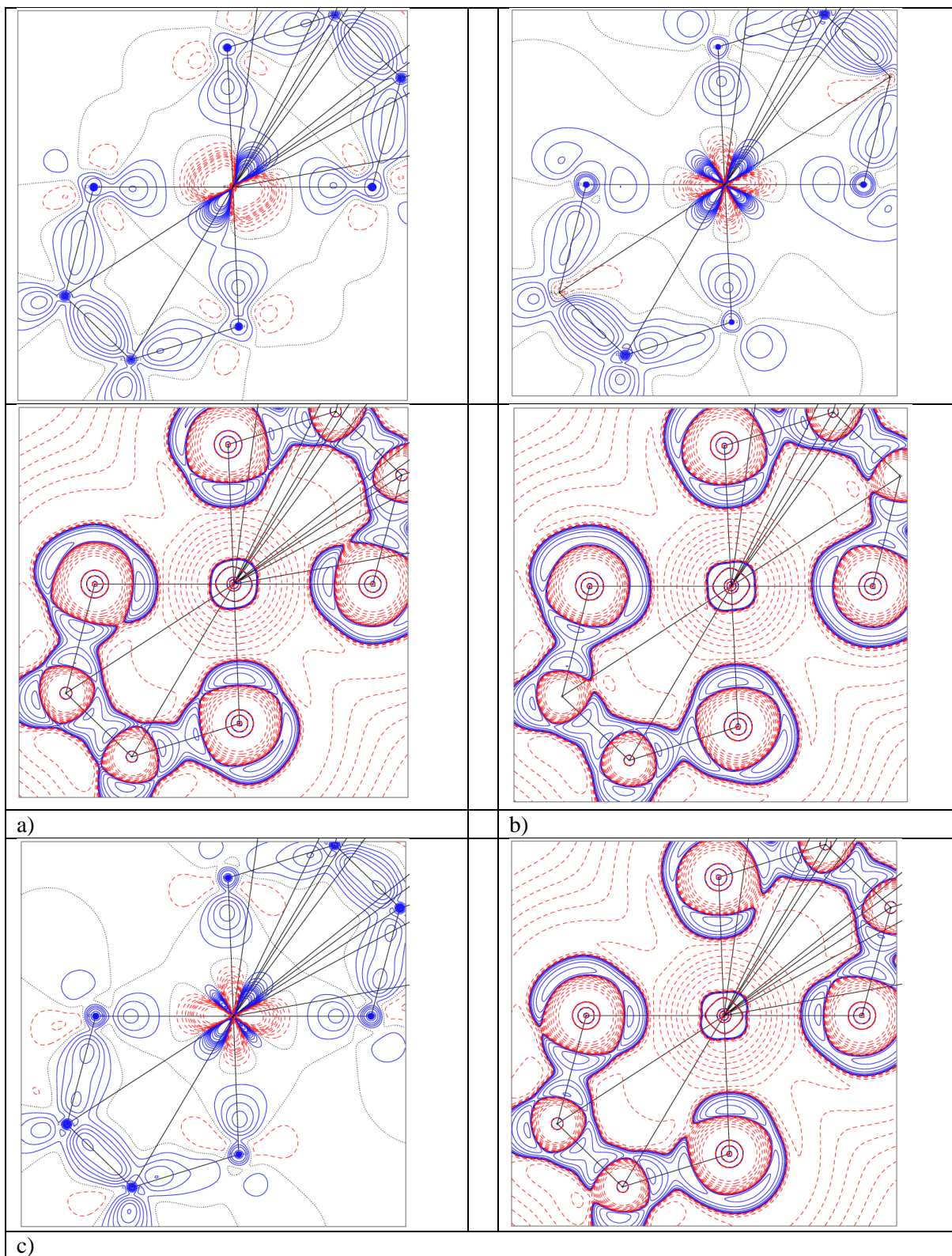
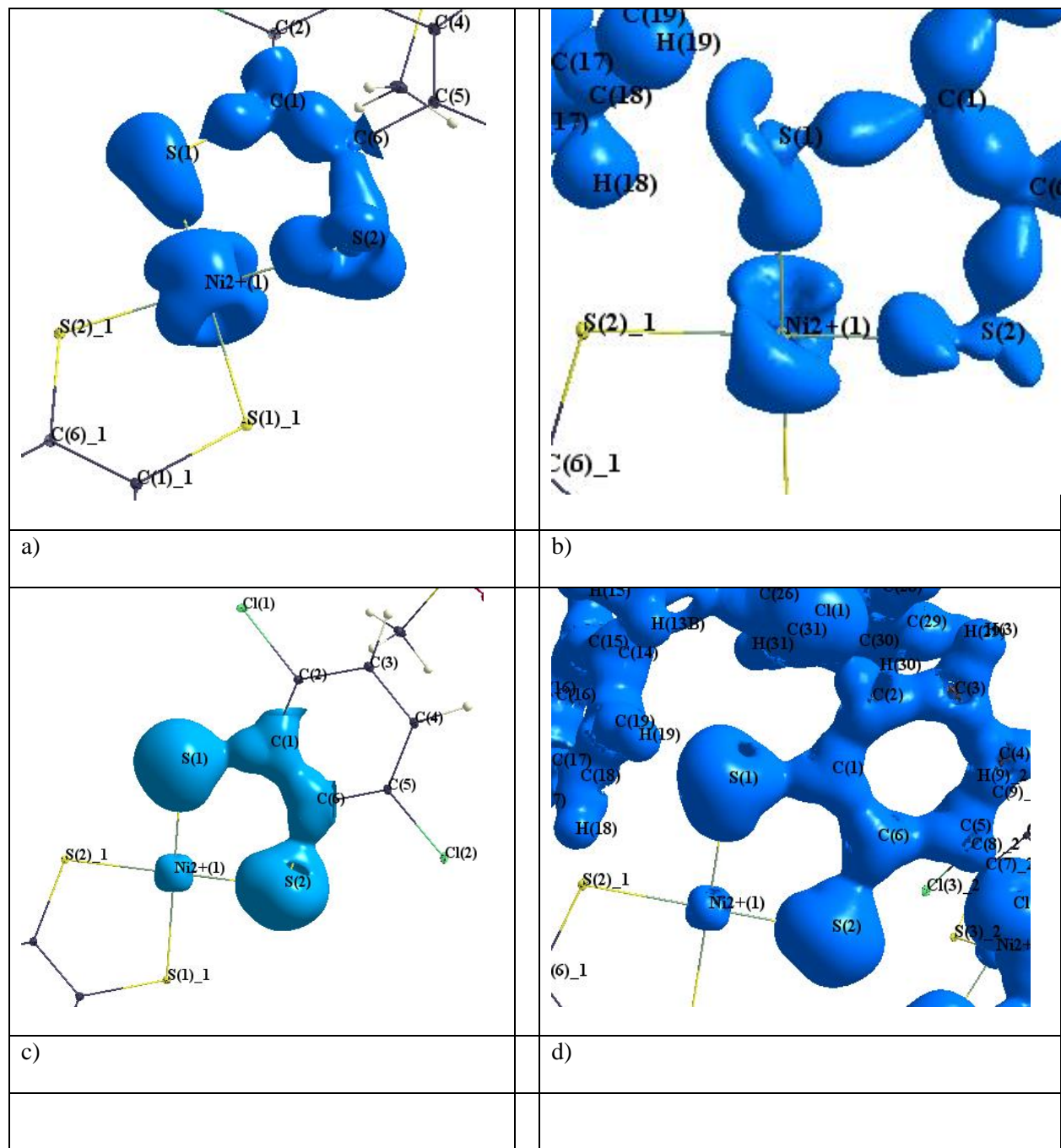


Figure S4. Experimental static electron deformation densities and Laplacian maps. Contours as in Figures S2. a) DD & Laplacian for (2) Ni2; b) DD & Laplacian for (2, 15 K) Ni1; c) DD & Laplacian for (2, 15 K) Ni2.



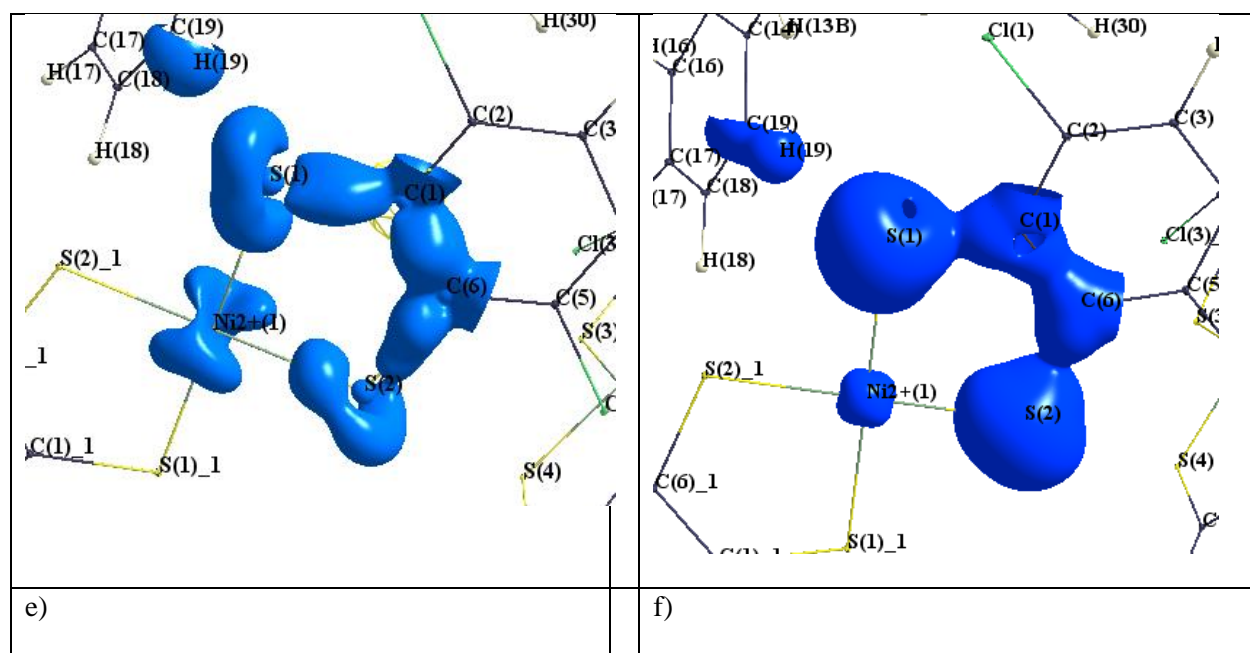


Figure S5. 3D plots of DDs and Laplacians at isovalue 0.1. a) DD for **(1)**; b) DD for **(2)** Ni1; c) Laplacian for **(1)**; d) Laplacian for **(2)** Ni1; e) DD for **(2, 15 K)** Ni1; f) Laplacian for **(2, 15 K)** Ni1

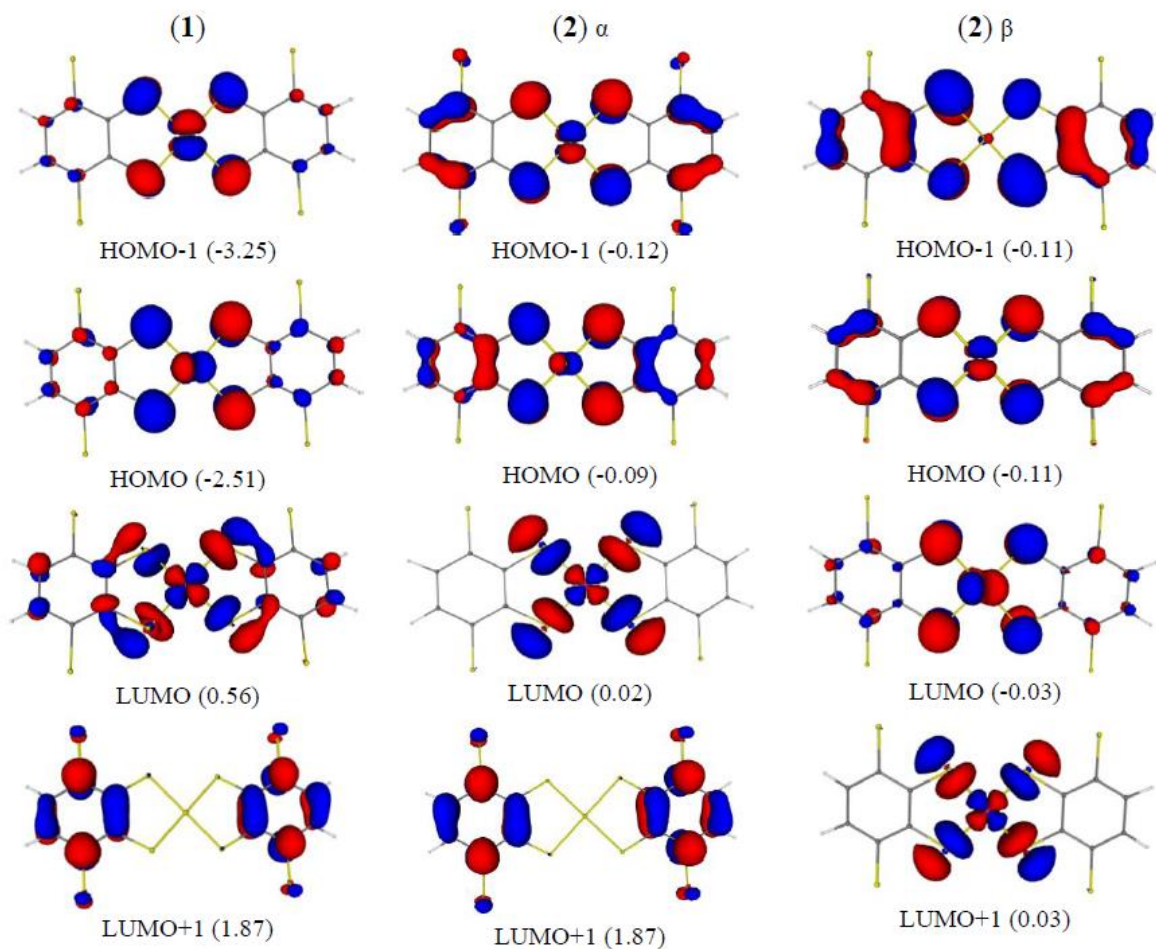


Figure S6. Frontier orbitals of studied complexes (eigenvalues are shown in parentheses in hartrees), the isosurface value is 0.04 e bohr^{-3}

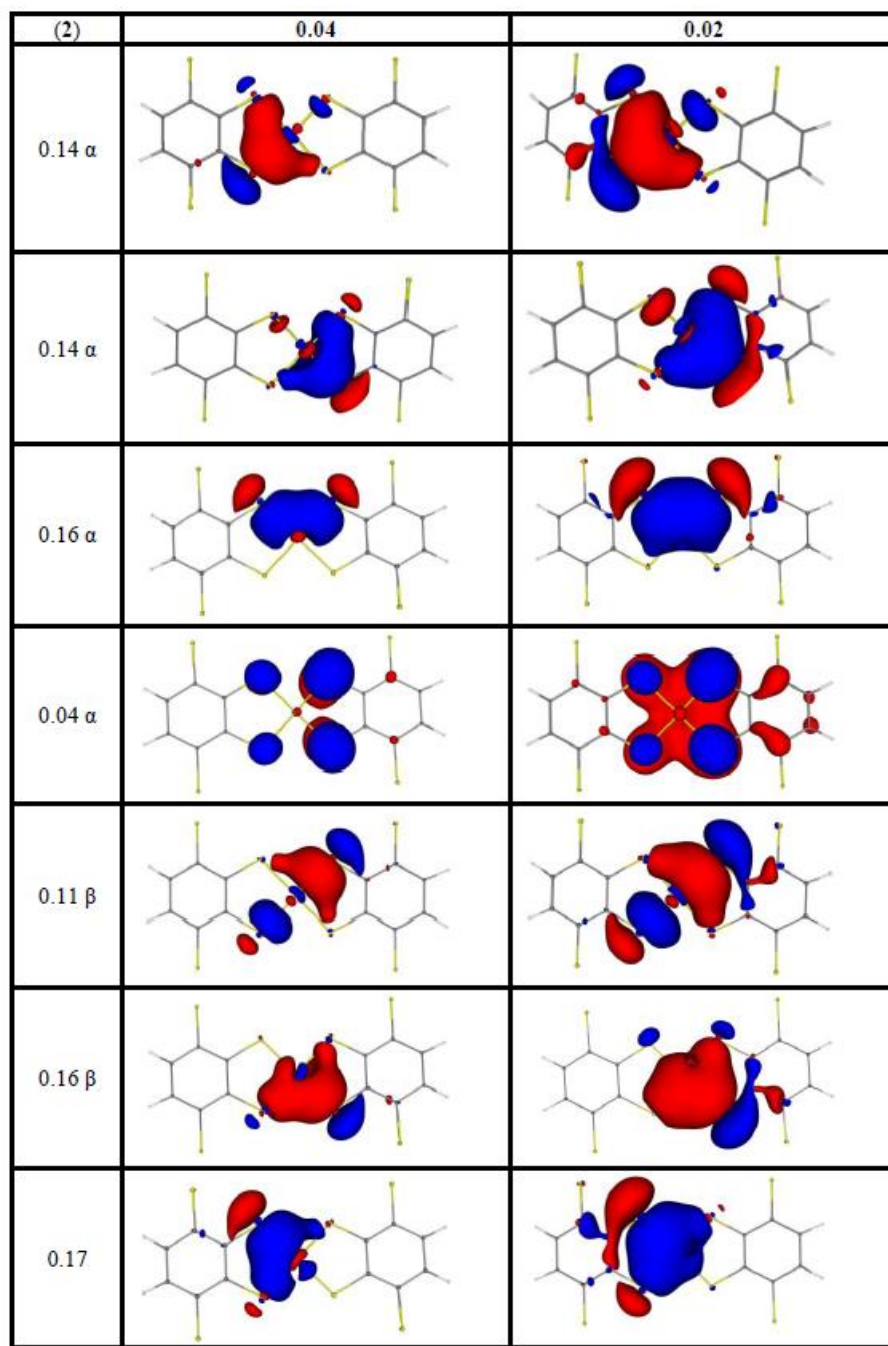


Figure S7. DAFH eigenvectors of **2** at the B3LYP/def2-TZVP level of theory (isovalue 0.04 and 0.02, red – negative, blue - positive). Ni atoms are chosen as the domain. The DAFH eigenvalues for the Ni basin/domain are shown in the left column.

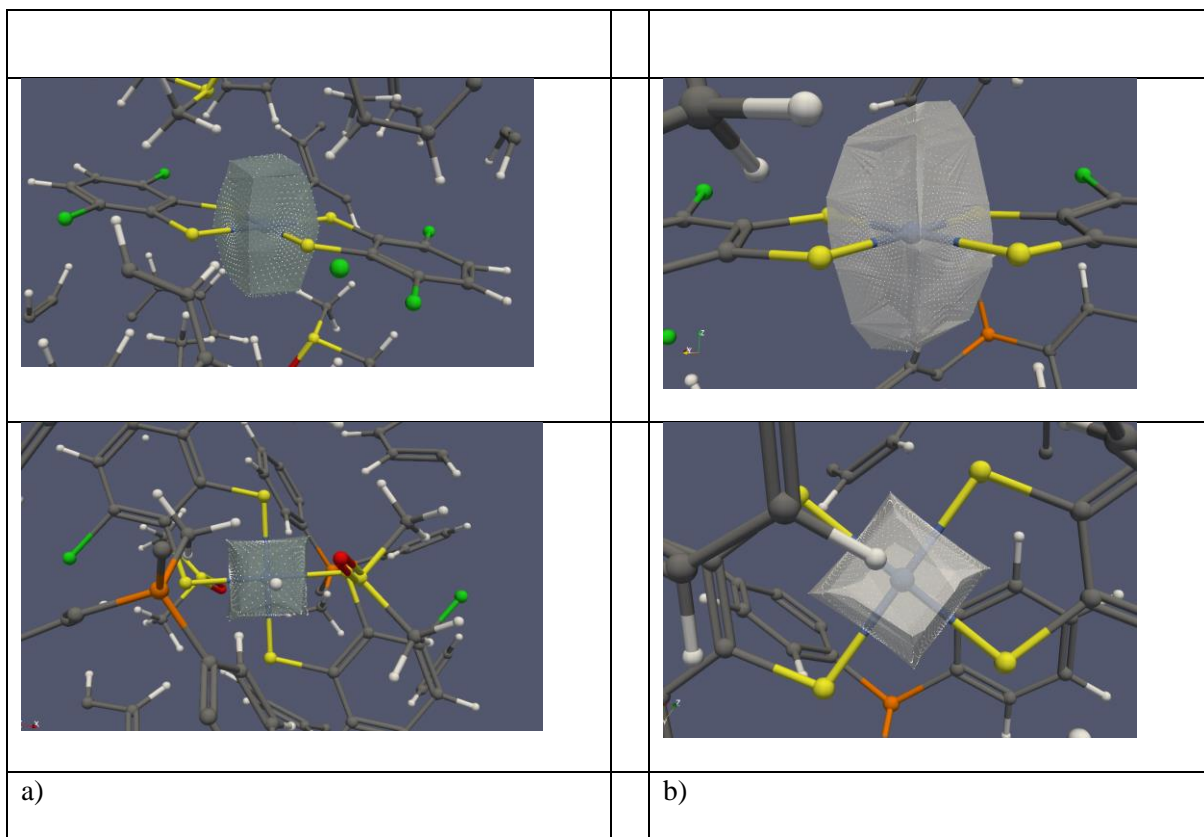


Figure S8. XDPROP, a) (1) VTOT = 11.554 Å³, Q = 0.737 e; b) (2) Ni(1); VTOT Ni(1) = 10.818 Å³, Q = 1.48 e; VTOT Ni(2) = 10.810 Å³, Q = 1.46 e.

References

- Ahrens, J., Geveci, B. & Law, C. (2005). *ParaView: An End-User Tool for Large Data Visualization*, *Visualization Handbook*, Elsevier.
- Ayachit, U. (2015). *The ParaView Guide: A Parallel Visualization Application*, Kitware.
- Gatti, C., Saunders, V. R. & Roetti, C. (1994). *J. Chem. Phys.* **101**, 10686 – 10696.
- Keith, T. A. & Bader, R. F. W. (1993). *J. Chem. Phys.* **99**, 3669-3682.
- Lebedev, V. I., Laikov, D. N. (1999) *Dokl. Math.* **59**, 477 - 481.
- Popelier, P.L.A. (1998). *Comput. Phys. Comm.* **108**, 180 - 190.
- Press, W.H., Teukolsky, S.A., Vetterling, W.T., Flannery, B.P. (1992) *Numerical Recipes in Fortran77. The Art of Scientific Computing*, 2nd edition, Cambridge University Press.
- Schreurs, A. M. M., Xian, X., Kroon-Batenburg, L. M. J. (2010). *J. Appl. Cryst.* **43**, 70-82.